# Ultrahydrophobic Polymer Surfaces Prepared by Simultaneous Ablation of Polypropylene and Sputtering of Poly(tetrafluoroethylene) Using Radio Frequency Plasma

**Jeffrey P. Youngblood and Thomas J. McCarthy*,†**

*Polymer Science and Engineering Department, University of Massachusetts, Amherst, Massachusetts 01003*

*Received March 8, 1999; Revised Manuscript Received June 16, 1999*

ABSTRACT: Ultrahydrophobic polypropylene surfaces were prepared by the simultaneous etching of polypropylene and etching/sputtering of poly(tetrafluoroethylene) (PTFE) using inductively coupled radio frequency argon plasma. The semicrystalline polypropylene surface is roughened due to the differential rates at which the crystalline and amorphous regimes ablate and is also fluorinated by the fluorocarbon plasma that results from the ablation/depolymerization of PTFE. The roughness of the polypropylene is controlled by the time of plasma etching. The presence of PTFE increases the rate of polypropylene roughening by reactive ion etching. The resulting roughened and fluorinated polypropylene surfaces were characterized by water contact angle, X-ray photoelectron spectroscopy (XPS), scanning electron microscopy, and atomic force microscopy (AFM). Wettability was found to depend on the size scale and topology of the roughness. The most hydrophobic surfaces exhibited advancing and receding water contact angles of $\theta_A/\theta_R = 172°/169°$.

## Introduction

The water repellency of a material is commonly measured by the contact angle that a water droplet makes with the surface. In thermodynamic terms, this is a measure of relative surface and interfacial energies and nothing else. True water repellency involves water droplets leaving surfaces or moving on surfaces—dynamic events in which thermodynamics may not be important. We recently reported[1] that the continuity of the air−solid−liquid contact line, which is determined by the topology of the roughness of the solid, is a critical parameter in determining hydrophobicity. The contact angle hysteresis (the difference between advancing and receding angles), that directly reflects the force required to move a drop on a surface[2] (and is controlled by the nature of the air−solid−liquid contact line) should be the most important criterion in judging hydrophobicity. We described[1] *ultrahydrophobic* and *ultralyophobic* surfaces (horizontal surfaces on which droplets are unstable and move easily) that exhibited low (or an apparent lack of) hysteresis, but not necessarily high contact angles.

That roughness can be important to hydrophobicity has long been recognized. In 1936, Wenzel[3] suggested that roughness has a major impact on the contact angle. His work demonstrated that, because the total energy is important, all of the surface under the drop must be considered. He introduced eq 1, where $\theta^{rough}$ is the

$$\cos \theta^{rough} = r \cos \theta \tag{1}$$

contact angle on a rough surface of a given material, $\theta$ is the thermodynamic contact angle on a smooth surface of that material, and $r$ is the roughness factor, where $r$ = actual surface area/geometric surface area. Cassie and Baxter[4] explained the wetting behavior of porous surfaces (having both liquid−air and liquid−solid interfaces), such as feathers and fabrics, and they proposed that at high levels of roughness, a fluid would sit primarily on the air contained in the pores of the rough material. They derived eq 2, where $\cos \theta^{porous}$ is the

$$\cos \theta^{porous} = f_1 \cos \theta - f_2 \tag{2}$$

apparent contact angle, $f_1$ is the fraction of fluid area in contact with the material, and $f_2$ is the fraction of the fluid area in contact with air in the porous material. Johnson and Dettre[5] predicted that a surface should transition sharply from a nonporous (Wenzel regime) to a porous surface (Cassie regime) as the roughness increases and that hysteresis should increase until this critical roughness is reached and then decrease. Their experiments[6] verify this, and they have commented on prior work that is consistent.[7] Subsequently, Garbassi et al.[8] published data that is consistent with the Johnson and Dettre theory. There have been numerous recent reports,[9−18] from a variety of research fields, of surfaces exhibiting very high water contact angles, due to surface topography. Each of these papers reports single water contact angles (not advancing and receding), so it is impossible to assess their true hydrophobicity. Surfaces that exhibit high advancing contact angles may exhibit low receding contact angles (we describe them as being in Wenzel's regime) so that drops may remain "pinned" to the surface, indicating poor water repellency.

We report here the preparation of ultrahydrophobic surfaces, which exhibit both high advancing and high receding water contact angles, by simultaneous etching of polypropylene and sputtering of poly(tetrafluoroethylene) (PTFE) using inductively coupled radio frequency argon plasmas. Plasma techniques have previously been reported to prepare nonwetting surfaces. Washo[19] reports contact angles of 165−170° for plasma-polymerized tetrafluoroethylene films, deposited in the powder region. Schreiber et al.[20] prepared plasma-polymerized hexamethyldisiloxane films using low-temperature

† tmccarthy@polysci.umass.edu

10.1021/ma9903456 CCC: $18.00 
Published on Web 09/18/1999

plasma deposition and measured water contact angles "as high as 180°." Garbassi et al.[8] examined the wettability of oxygen plasma-treated PTFE and report contact angles of $\theta_A/\theta_R$ = 170°/160°. This treatment of PTFE gives a rough, porous surface due to the difference in plasma susceptibility of crystalline and amorphous polymer;[21,22] crystalline regions etch more slowly than amorphous regions. Plasma sputtering of polymers[23−25] has been widely studied and is a momentum transfer process from the gas to the target, which dislodges molecular fragments that redeposit on the substrate. Sputtering of PTFE is anomalous[26−30] and progresses by decomposition to monomer, which then repolymerizes.

## Experimental Section

Plasma modification reactions were carried out in a previously described[31] home-built inductively coupled Pyrex reactor in which flow rate, power (13.56 MHz—supplied by an Astron RS-35A power supply and a Yaesu FT-840 HF transceiver), and pressure can be controlled. X-ray photoelectron spectra (XPS) were recorded on a Perkin-Elmer-Physical Electronics 5100 spectrometer with Al Kα excitation (15 kV, 400 W) at takeoff angles of 15 and 75° (between the plane of the sample and the entrance lens of the detector optics). Atomic concentration data were determined using sensitivity factors obtained from samples of known composition: $C_{1s}$, 0.200; $O_{1s}$, 0.501, $N_{1s}$, 0.352, $F_{1s}$, 1.00. Contact angle measurements were made with a Ramé-Hart telescopic goniometer and a Gilmont syringe with a 24-gauge flat-tipped needle. Dynamic advancing and receding angles were recorded as the probe fluid (either water, purified using a Millipore Milli-Q system that involves reverse osmosis followed by ion-exchange and filtration steps or hexadecane, purified by vacuum distillation) was added to and withdrawn from the drop, respectively. Atomic force microscopy (AFM) was performed in air using a Digital Instruments Nanoscope IIIa AFM in tapping mode. Scanning electron microscopy (SEM) micrographs were obtained with a JEOL-35CF microscope using an acceleration voltage of 20 kV.

Biaxially oriented capacitor grade polypropylene (6 μm thick) was obtained from Aerovox, Inc. PTFE film (4 mil) was obtained from Berghoff America. The polypropylene was cut into 1 in.$^2$ samples and placed into the full glow region of the plasma reactor on top of PTFE film (∼90 in.$^2$). The reactor was then sealed and evacuated to <0.01 mm. The chamber was then filled with argon (Merriam Graves) to a pressure of 5 mm and then pumped to a steady-state condition of 0.2 mm and 1.0 sccm. These conditions were held at the steady state for 30 min to ensure stability. The radio coil was then charged and the plasma was ignited (if needed) with an antistatic gun. Various times of reaction were studied at a power of 100 W. Analyses were carried out on the exposed side of the polypropylene.

## Results

**Surface Chemistry.** Polypropylene and PTFE (in surface area excess of ∼90 over polypropylene) film samples were simultaneously exposed to an argon plasma under conditions described in the Experimental Section. Both films are etched by the plasma; the etching of the PTFE produces a reactive fluorocarbon plasma that fluorinates the polypropylene surface in competition with its ablation. Figure 1 shows the atomic concentration of fluorine present in the surface region of polypropylene, determined by XPS, as a function of treatment time. Data for two takeoff angles are included. The 15° takeoff angle data indicate the composition of the outermost ∼10 Å, and the 75° takeoff angle data represent the composition of the outermost ∼40 Å.[32] In addition to carbon and fluorine, oxygen and nitrogen are also present in all samples. Samples reacted for 20 min or less contained ∼20 atom % oxygen and 1−2 atom % nitrogen (75° data). Samples reacted for 60 min or longer contained 1−2 atom % oxygen and 0.5−1.5% nitrogen (75° data). The 15° fluorine concentration plateaus above 40 atom % after 6 min and rises to above 50 atom % after 2 h (F:C ratios are ∼1.4:1). The 75° data show a similar trend, but concentration plateaus above 50 atom % fluorine after 20 min and rises to ∼60 atom % after 2 h (F:C ratios are ∼1.6:1). Several points concerning these data warrant comment: (1) The surfaces are highly fluorinated even at low reaction times and the surface composition of the polypropylene remains approximately the same after ∼20 min reaction. This indicates that solid PTFE is an excellent fluorinating agent in an argon plasma. (2) The 15° data (fluorine concentration) are higher than the 75° data at low reaction times and plateau earlier than the 75° data. This takeoff angle dependence and the reaching of plateau values indicate that samples treated for less than ∼20 min contain fluorinated polypropylene surface layers that are less than 40 Å thick and that samples treated for longer times have modified layers at least 40 Å thick. (3) The takeoff angle dependence for samples treated for times longer than 20 min is unusual, indicating that reaction is more extensive in the region beneath ∼10 Å deep than in the near-surface region. We ascribe this to reaction of radicals with oxygen after exposure of the sample to air. This is followed by elimination of HF (α-fluoro alcohols are unstable), reducing the fluorine content at the surface.

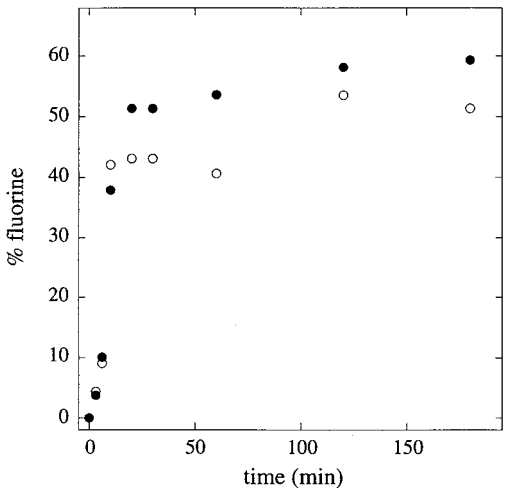


**Figure 1.** XPS atomic concentration of fluorine in polypropylene as a function of argon/PTFE plasma reaction time; ○, 15° takeoff angle, ●, 75° takeoff angle.

Contact angle is normally a useful technique for assessing changes in surface chemistry and conversion of a hydrocarbon surface to a fluorocarbon surface should be straightforward to follow using this method. Analysis of data from this system is complicated, however, because in addition to chemical changes, significant topographical changes occur (we chose this system for this reason). Topography is discussed in detail below. Figure 2 shows advancing and receding contact angle data (water) for polypropylene treated with argon/PTFE plasma for various durations. After short reaction times (less than 6 min), contact angles decrease from $\theta_A/\theta_R$ = 103°/89° to ∼58°/∼11°. There is not sufficient fluorination of the sample after this treatment duration (Figure 1) to hydrophobize the

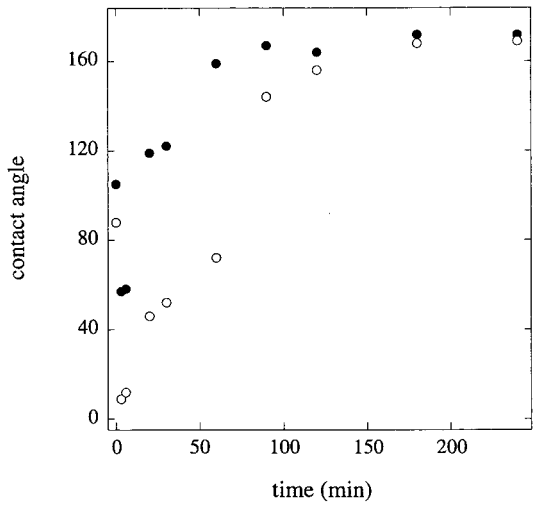


**Figure 2.** Advancing (●) and receding (○) contact angles of roughened and fluorinated polypropylene as a function of argon/PTFE plasma reaction time.

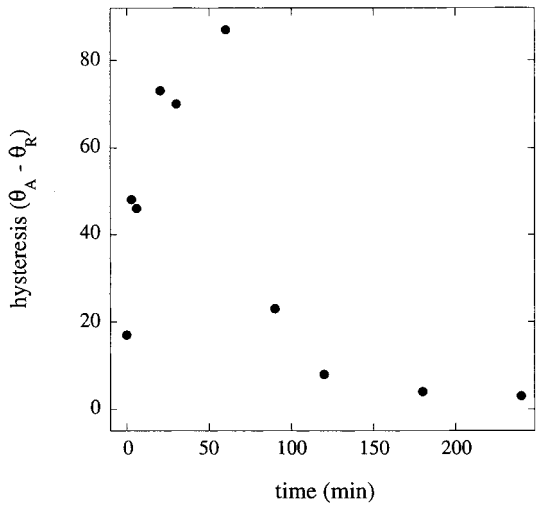


**Figure 3.** Contact angle hysteresis ($\theta_A - \theta_R$) of roughened and fluorinated polypropylene as a function of argon/PTFE plasma reaction time.

material; the decrease is likely due to two factors: (1) the presence of oxygen and nitrogen functionality (that is indicated by XPS) and (2) roughening. Wenzel's equation (eq 1) predicts a decrease in $\theta^{rough}$ with increasing roughness if the contact angle is less than 90° (cos $\theta$ is positive). After 20−30 min reaction time, the advancing contact angle is higher ($\theta_A = \sim 120°$) than the initial value for polypropylene ($\theta_A = 103°$), and it continues to rise to ∼170° with longer treatments. The receding contact angle rises with longer treatment time, but remains lower than the initial polypropylene value unless reaction times greater than 60 min are used; $\theta_R$ values converge on $\theta_A$ values after 3 h of reaction. The highest contact angles observed are $\theta_A/\theta_R = 172°/169°$.

This contact angle behavior is exactly what is predicted (with the exception of the initial decrease in $\theta_A$ due to polar functionality) by Johnson and Dettre[5] for a hydrophobic surface becoming rougher with reaction time. Surfaces that have been treated for 60 min or less exhibit high advancing contact angles and low receding contact angles (water drops are pinned on these surfaces); thus, water penetrates at least a significant percent of the valleys of the rough surface. We describe the rugosity of surfaces with this behavior as being in the Wenzel regime. Surfaces that have been treated for 90 min or longer exhibit both high advancing and receding contact angles. Water does not penetrate a significant percent of the valleys on these surfaces and contacts only the ridges (air is trapped in the valleys); water drops roll easily on horizontal surfaces. We describe these surfaces as *ultrahydrophobic* and term their rugosity as being in the Cassie regime. The water contact angle hysteresis is plotted vs time in Figure 3; a maximum is observed at 60 min reaction time and a sharp decrease occurs with further reaction. The roughness changes during this reaction period (60−90 min) are responsible for the transition from the Wenzel to the Cassie regime. None of the surfaces prepared by this method are *ultralyophobic*[1] as hexadecane drops remain pinned on them. Advancing hexadecane contact angles increase with reaction time to a plateau of ∼105°, but receding contact angles were 0° for all surfaces.

**Surface Topography.** Figure 4 shows a series of SEM micrographs of polypropylene samples that were treated with argon/PTFE plasma for different reaction times. Each has the same magnification. The surfaces become rougher with reaction time with the features becoming smaller, closer together and more contorted. We have not examined the cause of this roughening (in terms of the initial polypropylene morphology) and rationalize it as based on the different etching rates of crystalline and amorphous material. The same features are observed in argon plasma treated polypropylene samples (without PTFE present). The etching rate is significantly slower than with PTFE present, but resulting samples are indistinguishable, using SEM, from those prepared with argon/PTFE plasma treatments. A sample etched with argon for 120 min exhibited a roughness (Wenzel's $r$—see below) of 1.2. With PTFE present, a 120 min reaction rendered $r = \sim 3$. The morphologies are quite reproducible, but occasionally a very different morphology was observed. These samples exhibited hemisphere-shaped asperities; we ascribe this to melting and recrystallization of the polypropylene during treatment but have not examined the process in any detail or deliberately tried to make samples with this topography. Data from samples that exhibited these ball-like features were discarded. We note that a striking change in the size scale of the roughness occurs between 60 and 90 min of reaction. This coincides with (and we believe is responsible for) the abrupt rise in the receding contact angle and corresponding decrease in hysteresis observed (Figures 2 and 3).

Atomic force microscopy was carried out on this series of samples to quantitate the topography changes. The images and topographies are qualitatively similar and the dimensions of the features are quantitatively similar to those observed using SEM, but the quality of the data is poorer, due to transfer of polymer to the probe tip. AFM data was used to calculate two types of roughness, an average peak to valley distance and a ratio of surface area to geometric area (Wenzel's $r$). The latter was determined by squaring the ratio of the contour length to the straight-line length (20 $\mu$m) of a 20 $\mu$m $X-Z$ slice of the data. The effects of reaction time on these roughness values are plotted in Figure 5. The roughness increases gradually with reaction time and we emphasize that there is no sharp change in roughness that occurs between 60 and 90 min reaction time. Only data for samples reacted for 120 min or less are included;

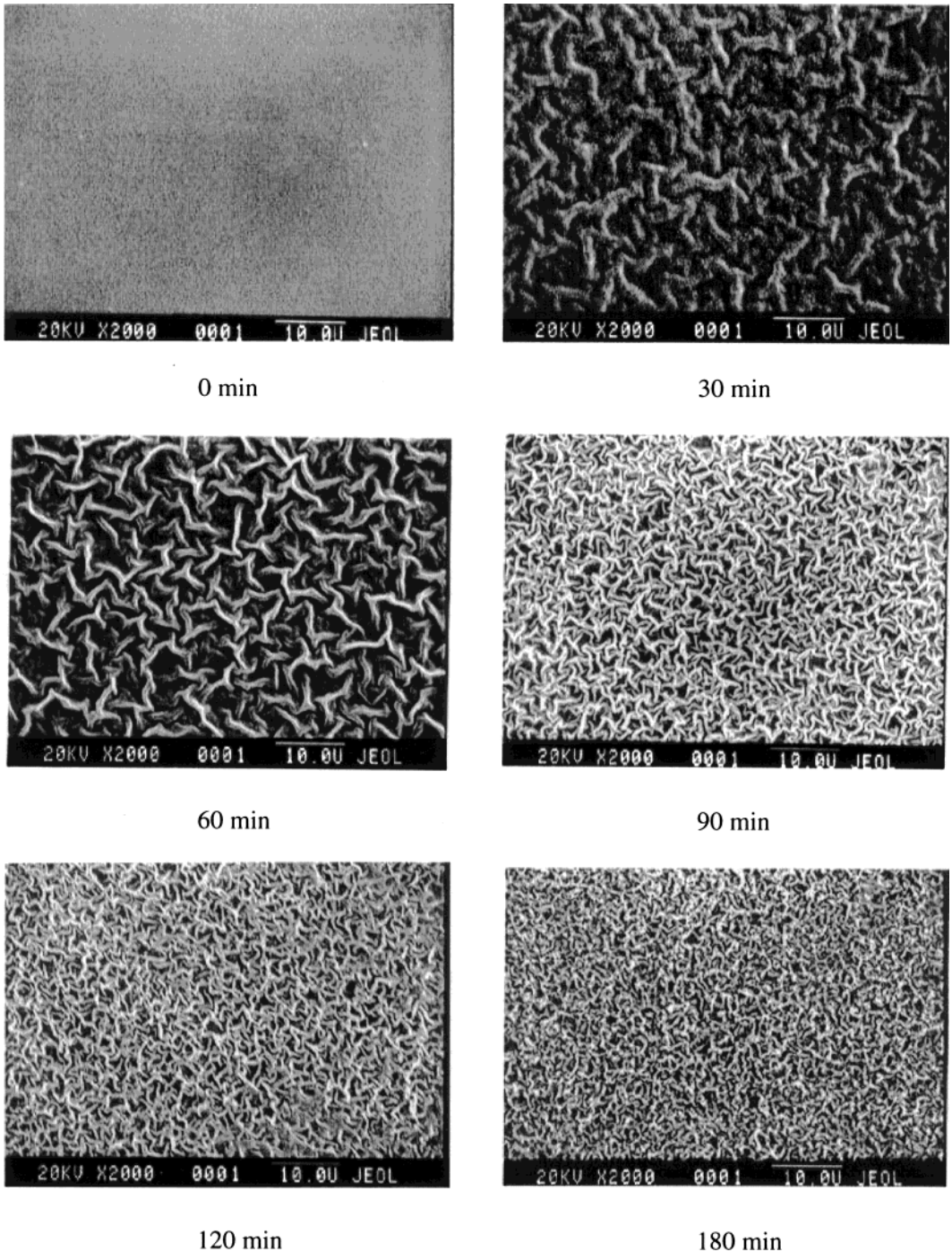


**Figure 4.** Scanning electron micrographs of polypropylene as a function of argon/PTFE plasma reaction time.

there was excessive error in samples reacted for longer times. Clearly there is a dramatic difference in the surface topography between the samples reacted for 60 and 90 min (Figure 4), but this is not reflected in the calculated roughness values.

**Relevance of Chemistry and Topography to Hydrophobicity.** Comparisons of Figures 1 and 2 and Figures 1 and 3 indicate that surface chemistry (fluorine content) is not responsible for the differences in wettability—contact angle and hysteresis—between samples treated with argon/PTFE plasma for 60 min or less and samples treated for 90 min or more. There is a striking difference in wettability between these two sets of surfaces that roughness is responsible for, and we will focus on two samples, those treated for 60 and 90 min. Water droplets stay pinned on 60-min-treated samples, even when the samples are tilted significantly from the horizontal. Water droplets, however, move spontaneously on horizontal surfaces of 90-min-treated samples and do not come to rest but roll off of the samples.

## Discussion

In order for a droplet of water, in contact with a solid surface, to move across that surface (spontaneously or due to an external force), it has to both advance and recede. The force required to start a drop moving on a surface is related to the difference between the advancing and receding contact angles (eq 3).[2] This implies that water droplets on surfaces that exhibit no water contact

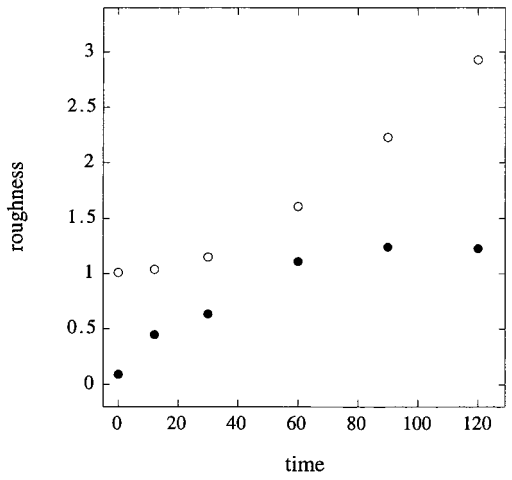


**Figure 5.** Peak to valley (●, in micrometers) and Wenzel's (○, ratio of surface area to geometric area) roughness values of polypropylene as a function of argon/PTFE plasma reaction time.

$$F = \gamma_L(\cos \theta_R - \cos \theta_A) \quad (3)$$

angle hysteresis will not be stable and will easily slide or roll, regardless of the magnitude of the contact angle. Thus, a surface with water contact angles of $\theta_A/\theta_R$ = 99°/99° should be considered more hydrophobic than a surface exhibiting contact angles of $\theta_A/\theta_R$ = 170°/100°.

When a droplet moves on a surface, the entire contact perimeter (three-phase liquid/solid/vapor contact line) must move. More important to the argument that we are about to make is that, for small movements or for each of many small incremental movements, the only liquid−solid interfacial water molecules that need to move are those that cover bare surface (upon advancing) and those that dewet the surface (upon receding). The other interfacial water molecules need not move. So the actions of wetting and dewetting or the actions of a droplet moving on a surface involve only contact line events and need not (and presumably do not) involve the vast majority of the liquid−solid interface. Consider the origin of hysteresis. When a drop deforms on a tilted surface prior to moving, the contact angles of the "downhill" 180° of the contact line increase and those on the "uphill" portion decrease (normally this is viewed in two dimensions with only two angles considered). There are energy barriers for both advancing and receding, and they may be (and most often will be) different. If the drop advances (at any point on or at all of the downhill contact line), before it recedes, this will induce an instability in the drop (increase in surface area at constant volume) that will cause recession. If the drop recedes first, this will introduce a different instability (a drop shape change due to gravity that will increase the advancing angle) that will cause advancement. When the drop is moving, both events must occur concertedly or in rapid succession, so whichever event, advancement or recession, has a higher energy barrier is not an important issue—neither is rate-limiting. We point out that instabilities at any point on the contact line (not just the advancing and receding "points") will contribute to the momentum of a moving droplet. These energy barriers that give rise to contact angle hysteresis are generally considered to arise from three sources: chemical heterogeneity, strong interaction between the water and the surface, and surface roughness. We are

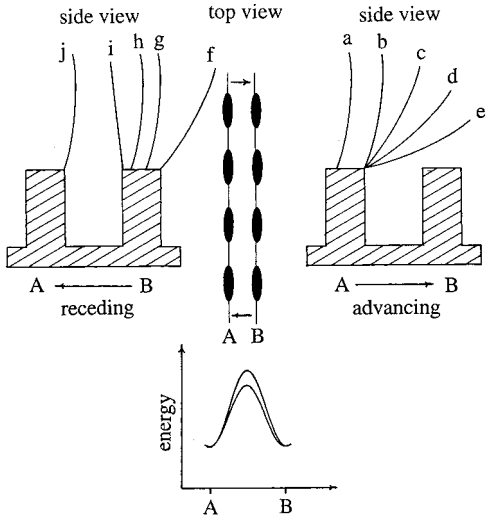


**Figure 6.** Pictorial representation of advancing and receding of a water droplet on a surface of model roughness that pins the water drop.

concerned here only with roughness and are considering only chemically homogeneous noninteracting surfaces.

Roughness is not a simple parameter to quantify (or to describe). We have demonstrated[33] that molecular scale (subnanometer) roughness contributes to contact angle hysteresis; that larger scale roughness also contributes has been shown many times. The amplitudes, periodicities, orientations, and topologies of roughness at multiple different length scales may be important. The issue that concerns us here is the following: At which length scales is roughness important to contact angle hysteresis? Consider a droplet at rest on a surface of some regular topography. We do not at this point want to address length scales, but if the drop diameter is measured in millimeters and the roughness scale is in micrometers, then the contact line at the roughness scale is a straight line at the drop diameter scale. Figure 6 describes a surface of one model roughness. The ellipses in the center of the figure describe plateaus that the water droplet rests on. We assume that water does not intrude into the valleys. This is a valid assumption because water will not intrude into micrometer scale pores of a hydrophobic surface at atmospheric pressures. Equation 4,[34] where $\Delta P$ is the hydrostatic pressure that

$$\Delta P = -p\gamma_L(\cos \theta_A)/A \quad (4)$$

must be exceeded before water will penetrate pores, $p$ is the perimeter of the pores, $\gamma_L$ is the surface tension of water, $\theta_A$ is the advancing contact angle of water on the surface, and $A$ is the area of the pore, is the governing expression; this equation predicts that pressures greater than 300 cm of water are necessary to cause intrusion into pores of micrometer size. The three-phase contact line of a drop on this surface will be in a position that maximizes its contact with the plateaus. This metastable state is indicated by line A in Figure 6. In order for this drop to advance to metastable state B, a large energy barrier has to be overcome (a force must be applied) as the contact line must jump across the valley. If water is added to the drop the contact line will be pinned at A (right side of figure) until the liquid−air interface "reaches down" and wets B. A near-180° advancing contact angle is predicted. In order for the drop to recede from B to A (left side of figure) a force

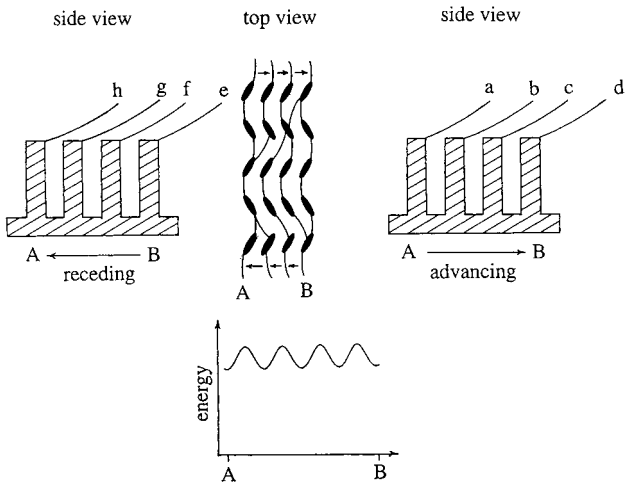


**Figure 7.** Pictorial representation of advancing and receding of a water droplet on an ultrahydrophobic surface of model roughness that does not pin the water drop.

must be applied as well. A different energy barrier must be overcome (we draw two lines in the energy diagram—see the bottom of the figure); If water is removed from the drop, the contact angle will decrease until the receding contact angle (of a smooth sample of the same material) is reached before receding. A lower angle may be observed due to pinning (i in the figure), and deformation of the drop (increasing the surface area-to-volume ratio) is required to overcome this barrier.

Figure 7 shows a model surface of different roughness. Again the ellipses indicate plateaus that the droplet rests on and the valleys are not penetrated. Metastable state A is much different and much less stable than that indicated in Figure 6. Here the contact line is less continuous, makes less contact with solid and more with air and has to distort from linear to maximize contact with the plateaus. This metastable contact line is higher in energy than that indicated in Figure 6 and is likely dynamic, shifting constantly (advancing and receding) even with the drop "at rest." To advance from A to B, the contact line can make several movements with much lower energy barriers than that described in Figure 6. Drop movement on a surface like this will involve many small reversible incremental advancements and recessions.

Figures 6 and 7 are meant as models for the polypropylene surfaces treated with argon/PTFE plasma for 60 and 90 min, respectively. Figure 8 shows higher magnification SEM micrographs of these surfaces. The features in the 60-min-reacted sample are larger, further apart and less contorted than those of the 90-min-reacted sample. The 60-min sample exhibits relatively wide (0.5−1 $\mu$m) ridges with straight or gradually curving sections of ~5 $\mu$m that are spaced by several micrometers. The 90-min sample exhibits thinner, much more contorted ridges that are spaced by a micrometer or less. Envisioning the features in these micrographs as the "plateaus" of Figures 6 and 7, the three-phase contact lines on the 90-min samples will be less continuous, more contorted, and less stable, and the barriers between metastable states will be lower than those of the 60-min samples. Although we cannot determine which parts of these surfaces will be in contact with water at the three-phase contact line, it is likely that water penetrates portions of some of the valleys of the 60-min sample. The lower (almost absence of) hysteresis

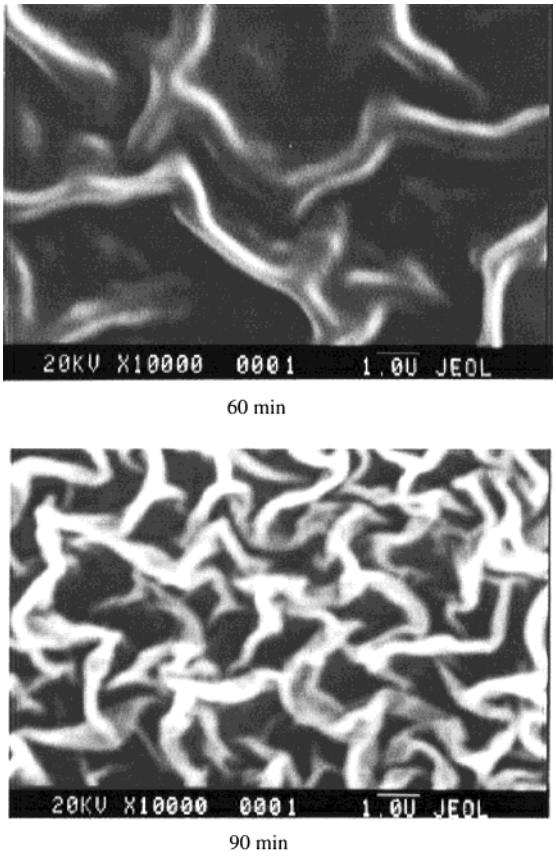


**Figure 8.** Higher magnification scanning electron micrographs of polypropylene samples treated with argon/PTFE plasma for 60 and 90 min.

observed in samples treated for 90 min or more is due to both an increase in the ground-state energy of the metastable states and a decrease in the energy barriers between metastable states.

## Summary

Biaxially oriented polypropylene was simultaneously roughened and fluorinated using an inert gas plasma and PTFE as a solid phase reactant. The ablation rate of polypropylene is enhanced by the PTFE, presumably due to reactive ion etching caused by fragmented TFE species. Reaction time can be used to control the nature of the surface roughness; features become smaller, more pronounced, more contorted and closer together with increasing reaction time. After a critical reaction time (between 60 and 90 min), the surfaces become ultrahydrophobic—water droplets roll easily on horizontal surfaces. Contact angles are as high as $\theta_A/\theta_R = 172°/169°$, and hysteresis is very low. We explain this ultrahydrophobicity in terms of the shape and continuity of the three-phase (liquid/solid/vapor) contact line. Metastable states for the droplets are high in energy, and the barriers between metastable states are low.

**Acknowledgment.** We would like to thank the Office of Naval Research and the NSF-sponsored Materials Research Science and Engineering Center for financial support.

## References and Notes

(1) Chen, W.; Fadeev, A. Y.; Hsieh, M. C.; Öner, D.; Youngblood, J. P.; McCarthy, T. J. *Langmuir* **1999**. *15*, 2295.

(2) Wolfram, E.; Faust, R. in *Wetting, Spreading and Adhesion*; Padday, J. F., Ed.; Academic Press: London, 1978; p 213.
(3) Wenzel, R. N. *Ind. Eng. Chem.* **1936**, *28*, 988.
(4) Cassie, A. B. D.; Baxter, S. *Trans. Faraday Soc.* **1944**, *3*, 16.
(5) Johnson, R. E., Jr.; Dettre, R. H. *Adv. Chem. Ser.* **1964**, *43*, 112.
(6) Dettre, R. H.; Johnson, R. E., Jr. *Adv. Chem. Ser.* **1964**, *43*, 136.
(7) Bartell, F. E.; Shepard, J. W. *J. Phys. Chem.* **1953**, *57*, 211.
(8) Garbassi, F.; Morra, M.; Occhiello, E. *Langmuir* **1989**, *5*, 872.
(9) Onda, T. Shibuichi, S.; Satoh, N.; Tsujii, K. *Langmuir* **1996**, *12*, 2125.
(10) Shibuichi, S.; Onda, T.; Satoh, N.; Tsujii, K. *J. Phys. Chem.* **1996**, *100*, 19512.
(11) Tadanaga, K.; Katata, N.; Minami, T. *J. Am. Ceram. Soc.* **1997**, *80*, 1040.
(12) Tadanaga, K.; Katata, N.; Minami, T. *J. Am. Ceram. Soc.* **1997**, *80*, 3213.
(13) Veeramasuneni, S.; Drelich, J.; Miller, J. D.; Yamauchi, G. *Prog. Org. Coat.* **1997**, *31*, 265.
(14) Ogawa, K.; Soga, M.; Takada, Y.; Nakayama, I. *Jpn. J. Appl. Phys. Part. 2: Lett.* **1993**, *32*, L614.
(15) Kunugi, Y.; Nonaku, T.; Chong, Y. B.; Watanabe, N. *J. Electroanal. Chem.* **1993**, *353*, 209.
(16) Schakenraad, J. M.; Stokroos, I.; Bartels, H.; Busscher, H. J. *Cells Mater.* **1992**, *2*, 193.
(17) Hozumi, A.; Takai, O. *Thin Solid Films* **1997**, *303*, 222.
(18) Miller, J. D.; Veeramasuneni, S.; Drelich, J.; Yalamanchili, M. R.; Yamauchi, Y. *Polym. Eng. Sci.* **1996**, *36*, 1849.
(19) Washo, B. D. *Org. Coat. Appl. Polym. Sci. (Am. Chem. Soc.)* **1982**, *47*, 69.
(20) Sacher, E.; Klemberg-Sapieha, J.; Schreiber, H. P.; Wertheimer, M. R.; McIntyre, N. S. In *Silanes, Surfaces, and Interfaces*; Leyden, D. E., Ed.; Gordon and Breach: New York, 1986; p 189.
(21) Yasuda, T.; Yasuda, H.; Okuno, T.; Miyama, M. *Polym. Mater. Sci. Eng. (Am. Chem. Soc.)* **1990**, *62*, 457.
(22) Dwight, D. W.; McCartney, S. R. F. *Org. Coat. Appl. Polym. Sci. (Am. Chem. Soc.)* **1984**, *50*, 459.
(23) Robertson, T.; Morrison, D. T. *Thin Solid Films* **1973**, *15*, 87.
(24) White, M. *Thin Solid Films* **1973**, *18*, 157.
(25) Davidse, P. D.; Maissel, L. I. *J. Appl. Phys.* **1966**, *37*, 574.
(26) Golub, M. A.; Wydeven, T.; Johnson, A. L. *Langmuir* **1998**, *14*, 4, 2217.
(27) Ryan, M. E.; Badyai J. P. S. *Macromolecules* **1995**, *28*, 1377.
(28) Pratt, I. H.; Lausman, T. C. *Thin Solid Films* **1972**, *10*, 151.
(29) Tibbitt, J. M.; Shen, M.; Bell, A. T. *Thin Solid Films* **1975**, *29*, L43.
(30) Mathias, E.; Miller, G. H. *J. Phys. Chem.* **1967**, *71*, 2671.
(31) Hsieh, M. C.; Farris, R. J.; McCarthy, T. J. *Macromolecules* **1997**, *30*, 8453.
(32) The relative XPS sampling depths for the two takeoff angles (1:4) are accurate, but the precise values (10 and 40 Å) are estimates, which depend on the $F_{1s}$ photoelectron mean free path in this material (which is unknown).
(33) Fadeev, A. Y.; McCarthy, T. J. Langmuir **1999**, *15*, 3759.
(34) Dettre, R. H.; Johnson, R. E. *Wetting*; S.C.I. Monograph No. 25; Society of Chemical Industry, London, 1967; p 144.

MA9903456